Analyst

RSC Publishing

PAPER

View Article Online
View Journal | View Issue

Cite this: *Analyst*, 2013, **138**, 1764

Microspectroscopic SERS detection of interleukin-6 with rationally designed gold/silver nanoshells†

Yuling Wang, Mohammad Salehi, Max Schütz, Katharina Rudi and Sebastian Schlücker*

Rationally designed gold/silver nanoshells (Au/Ag-NS) with plasmon resonances optimized for red laser excitation in order to minimize autofluorescence from clinical samples exhibit scattering cross-sections, which are *ca.* one order of magnitude larger compared with solid quasi-spherical gold nanoparticles (Au-NPs) of the same size. Hydrophilic stabilization and sterical accessibility for subsequent bioconjugation of Au/Ag-NS is achieved by coating their surface with a self-assembled monolayer (SAM) of rationally designed Raman reporter molecules comprising terminal mono- and tri-ethylene glycol (EG) spacers, respectively. The stability of the hydrophilically stabilized metal colloid was tested under different conditions. In contrast to metal colloids coated with a SAM without terminal EG spacers, the hydrophilically stabilized SERS particles do not aggregate under physiologically relevant conditions, *i.e.*, buffer solutions with high ionic strength. Using these rationally designed SERS particles in conjunction with a microspectroscopic acquisition scheme, a sandwich immunoassay for the sensitive detection of interleukin-6 (IL-6) was developed. Several control experiments demonstrate the high specificity of the assay towards IL-6, with a lowest detectable concentration of *ca.* 1 pg mL^{-1}. The signal strength of the Au/Ag-NS is at least one order of magnitude higher compared with hydrophilically stabilized, non-aggregated solid quasi-spherical Au-NPs of the same size.

Received 5th November 2012
Accepted 18th January 2013

DOI: 10.1039/c3an36610c

www.rsc.org/analyst

Introduction

Surface enhanced Raman scattering (SERS) is an emerging technique for the selective detection of biomolecules such as peptides, proteins and nucleic acids.[1–3] The advantages of SERS as a labeling/read-out approach include its reduced susceptibility to photobleaching, narrow vibrational Raman bands for spectral multiplexing, and high sensitivity.[4–6] SERS immunoassays are a potential alternative to enzyme-linked immunosorbent assays (ELISA). Their capability for sensitive and multiplexed protein detection has been demonstrated by Porter and co-workers[7–11] and Ozaki and co-workers.[12–14] A typical SERS immunoassay for protein detection is based on the sandwich immunocomplex, in which the capture antibodies are immobilized on a substrate such as glass coated with a thin gold film[8–10] and magnetic beads/nanoparticles.[15,16] The corresponding antigen is captured from the sample solution and detected *via* the characteristic Raman spectrum of the SERS-labeled detection antibody after the formation of the sandwich. Quantitative information is obtained from concentration-dependent SERS experiments. The sensitivity and the reproducibility of SERS-based assays are strongly dependent on the quality of the SERS labels in terms of signal strength and colloidal stability. Porter and co-workers have introduced SERS labels for protein detection comprising gold nanoparticles (Au-NPs) coated with a self-assembled monolayer (SAM) of arylthiols as Raman reporter molecules (Fig. 1A). A SAM offers the advantages of a maximum coverage of Raman label molecules on the metal surface, minimized co-adsorption of other molecules from the environment on the metal surface, and a uniform molecular orientation with respect to the surface normal for uniform Raman signal enhancement.[7–11] Potential drawbacks of this approach are that the colloidal stability depends on the particular type of Raman reporter molecule; terminal charges, for instance, are beneficial for preventing aggregation *via* electrostatic repulsion between colloidal particles. Further, a reduced sterical accessibility for the conjugation of large biomolecular ligands is a direct consequence of the dense packing of the Raman labels within the SAM. The rationally designed SERS labels depicted in Fig. 1B overcome both limitations. Monoethylene glycol spacers with a terminal hydroxyl group (MEG–OH) and triethylene glycol spacers with a terminal carboxyl group (TEG–CO_2H) for subsequent bioconjugation are covalently bound to an arylthiol as the actual Raman reporter moiety (Scheme 1A). Sterical accessibility is ensured by using an excess (typically 100 : 1 or 1000 : 1) of the Raman label–spacer conjugate with the shorter MEG–OH spacer (Fig. 1B and Scheme 1A).[17–20] The benefits of using MEG–OH and

Department of Physics, University of Osnabrück, Barbarastraße 7, 49069 Osnabrück, Germany. E-mail: sebastian.schluecker@uos.de

† Electronic supplementary information (ESI) available: Additional information as noted in text. See DOI: 10.1039/c3an36610c

TEG–CO_2H as hydrophilic spacers attached to aromatic Raman labels include the increased stability of the SERS labels due to the EG termini and the controllable bioconjugation *via* the MEG–OH/TEG–CO_2H stoichiometry, together with the advantages of a SAM (maximum surface coverage with Raman reporters, uniform molecular orientation, and minimal coadsorption of other molecules from the surrounding onto the metal surface).

SERS immunoassays have been reported for the detection of cell surface antigens,[21] immunoglobulin G (IgG),[8,13] protein A,[22] prostate-specific antigen (PSA)[9] and proteins against bacteria.[23] Cytokines are a diverse group of low molecular weight (generally <20 kDa) proteins, which are involved in a broad spectrum of biological functions. These functions include mediation or regulation of immune-responses.[24,25] Since these powerful regulatory and communication molecules are involved in the pathogenesis of disease, there is an increased demand for their detection at clinically relevant concentrations.[25] For example, Graham and co-workers achieved the sensitive detection of tumor necrosis factor α (TNF-α) with resonance Raman (RR) spectroscopy.[26] In the present study, interleukin-6 (IL-6) was chosen as a representative cytokine target because it is an inflammatory cytokine relevant to many disease processes[27] such as diabetes,[28] Alzheimer's disease,[29] prostate cancer[30] and rheumatoid arthritis.[31] It has been reported that advanced/metastatic cancer patients have higher median levels of IL-6 in their blood (14.8 pg mL^{-1} *vs.* 3.7 pg mL^{-1}).[32] The detection limit for IL-6 using conventional ELISA is about 18.7 pg mL^{-1},[33] which does not meet the requirements of clinical diagnostics. Improved detection limits have been reported for fluorescence[34] and surface plasmon resonance (SPR) sensing.[35] SERS, however, offers the additional unique spectral multiplexing advantage.

In this contribution, we employ hydrophilically stabilized Au/Ag-NS as rationally designed SERS labels (Fig. 1B) for the sensitive and reproducible detection of IL-6, using a sandwich immunoassay on functionalized glass slides in combination with a spatially resolved microspectroscopic detection scheme. The stability of the hydrophilic SERS labels was investigated under different physiologically relevant conditions including high salt concentrations and compared to metal colloids without terminal EG spacers conjugated to the SAM. The lowest detectable concentration of IL-6 using the hydrophilically stabilized Au/Ag-NS is compared with that using hydrophilically stabilized, nonaggregated solid quasi-spherical Au-NPs of the same size.

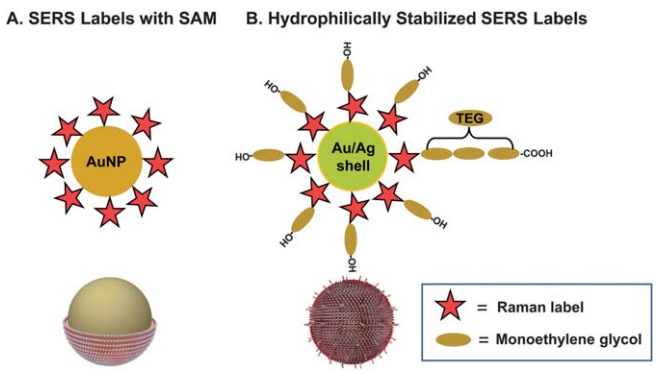

Fig. 1 Schematic illustration of SERS labels comprising Au-NPs coated with a SAM of Raman reporter molecules (A) and hydrophilically stabilized Au/Ag-NS (B).

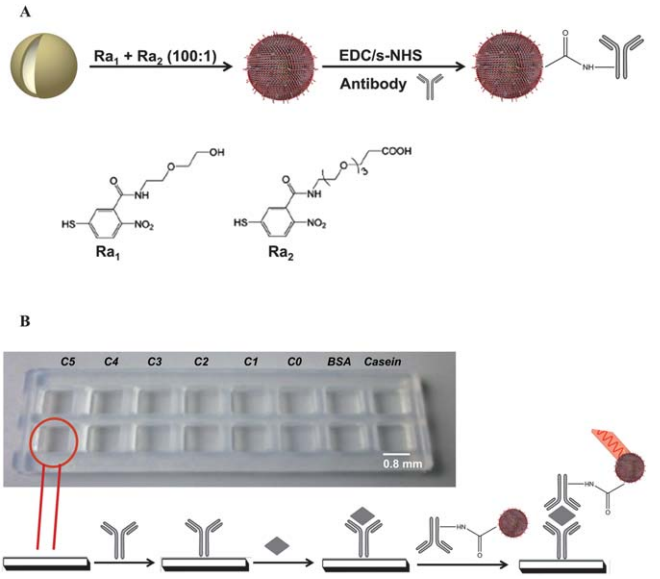

Scheme 1 (A) Synthesis of hydrophilically stabilized Au/Ag-NS labeled with antibodies; and (B) a sandwich SERS immunoassay platform for IL-6 detection.

Experimental

Reagents

5,5′-Dithiobis(2-nitrobenzoic acid) (DTNB), *N*-(3-dimethyl-aminopropyl)-*N*′-ethyl-carbodiimide (EDC), *N*-hydroxy-sulfosuccinimide sodium salt (s-NHS), $AgNO_3$, and $HAuCl_4$ were purchased from Sigma/Aldrich/Fluka. $NaHCO_3$, NaCl, Na_2HPO_4, KH_2PO_4, sodium acetate hydrate, ethanol, anhydrous ethylene glycol, polyvinylpyrrolidone (PVP), bovine serum albumin (BSA), tris (tris(hydroxymethyl)aminomethane) and HEPES (4-(2-hydroxyethyl)-1-piperazineethanesulfonic acid) were purchased from Carl Roth, Germany. Covalent conjugation of DTNB to a short monoethylene glycol (MEG–OH) and a longer triethylene glycol moiety (TEG–CO_2H) group was synthesized according to our previous report.[18] Monoclonal anti-human IL-6 antibody (MAB2061), human IL-6 affinity purified polyclonal antibody (AF-206-NA) and recombinant human IL-6 (206-IL-010) were purchased from R&D systems Inc. PBS buffer with pH = 7.4 was prepared according to standard protocols, using 137 mM NaCl, 2.7 mM KCl, 10 mM $Na_2HPO_4 \cdot 2H_2O$ and 2.0 mM KH_2PO_4.

Preparation of antibody–SERS label conjugates

Au/Ag-NS were prepared based on the template-engaged replacement reaction between silver nanoparticles and $HAuCl_4$ according to the method reported by Xia and co-workers.[36,37] Au-NPs with the same size (60 nm) were purchased from BBI. As-prepared Au/Ag-NS and Au-NPs were incubated with Raman reporters (DTNB–MEG–OH : DTNB–TEG–CO_2H = 100 : 1) at

room temperature (RT) under shaking for several hours to form the corresponding SAM on the metal surface as depicted in Scheme 1A. After incubation, the SAM-coated Au/Ag-NS and Au-NPs were centrifuged at 1920 *g* for 15 min and then re-dispersed into 500 μL of HEPES buffer (pH = 5.9). Afterwards, the carboxyl groups of the SERS labels (TEG–CO_2H) were activated by EDC/s-NHS (40 μL, 5 mg/1.5 mL EDC and 40 μL, 3 mg/1.5 mL s-NHS) in HEPES buffer at RT for 20 min under shaking. The SERS labels were then centrifuged to remove excess EDC/s-NHS and re-dispersed into 500 μL of HEPES buffer. 0.5 μg of polyclonal antibody (PAb) was then added to 500 μL of colloid containing activated SERS label suspension for reacting at RT for 1 h and at 4 °C overnight for the formation of antibody–SERS label conjugates. The maximum number of antibodies bound to the Au/Ag-NS surface was roughly estimated to be *ca.* 415 per nanoshell.[14] Then 400 μL of TT (Tris–Tween 20)-0.2% BSA buffer was added into 500 μL of suspension with SERS-labeled antibodies for reacting at RT for 15–20 min under shaking to block the particle surface from minimizing non-specific binding. After the reaction, the SERS-labeled antibodies were washed three times with TT-0.2% BSA buffer and centrifuged at 1920 *g* for 15 min at 6 °C. Then the SERS-labeled antibodies were re-dispersed into 500 μL of TT-0.2% BSA buffer and used for binding to the functionalized glass surface. The bioconjugation of antibodies to the SERS labels was tested by ELISA using a mouse monoclonal secondary antibody to Goat IgG-Fc HRP (ab99710 from Abcam) labeled with HRP (horseradish peroxidase). The enzyme substrate was *o*-phenylenediamine dihydrochloride (OPD). The absorbance of the colored reaction product was detected at 492 nm with a microplate reader (Sunrise™, TECAN. Ltd) after the enzymatic reaction was stopped with 3 M H_2SO_4.

Sandwich assay on HD glass slides

The SERS immunoassay platform is shown in Scheme 1B. High density (HD) TRIDIA™ (SurModics. Co) glass slides (see ESI, Fig. S2†) were used as the substrate for immobilization of the capture antibody. 16 separate compartments (see Scheme 1B) were generated by covering the functionalized glass surface with a structured, flexible polymer cover (Flexwell™, Grace Bio-Labs Inc.). The concentrations of the monoclonal antibody on the glass slide for binding were optimized to be 2 μg mL^{-1} according to the activity of HRP determined with a microplate reader (see above). The HD glass surface was incubated with 80 μL of 2 μg mL^{-1} monoclonal antibody dissolved in carbonate buffer I (CBI) buffer (0.2 M $NaHCO_3$ and 0.5 M NaCl with pH = 8.5) at RT for 1 h and 4 °C overnight. The glass surface was washed (vortexed) with carbonate buffer II (CBII) buffer (0.1 M $NaHCO_3$ and 0.5 M NaCl with pH = 8.0) three times, acetate buffer (AB) (0.1 M sodium acetate with pH = 4.4) once and PBST buffer (PBS with 0.05% Tween 20, pH = 7.4) once. Then the glass slides were blocked by 2% BSA solution at RT for 2 h to minimize nonspecific binding. The slides were then washed (vortexed) with PBST three times. After that, different concentrations of antigen ranging from 0 pg mL^{-1} to ~1 μg mL^{-1} or 2% BSA, 2% casein and 1 μM protein G as negative controls were incubated with the glass slide at RT for 1 h and then kept at 4 °C overnight. The glass slides were washed three times again with PBST buffer and then incubated with SERS-labeled antibodies at RT for 1 h and at 4 °C overnight. The concentration of SERS labels added for incubation was normalized each time to the optical density of the colloid to ensure reproducibility. Afterwards, the glass slides were washed three times with PBST and dried under a nitrogen atmosphere for the measurement.

Instrumentation

Au/Ag-NS were characterized by transmission electron microscopy (TEM) (Zeiss, EM 902) and UV-Vis extinction spectroscopy (Perkin Elmer, Lambda 35). SERS spectra were recorded with a WITec alpha 300 R microspectrometer. The 632.8 nm line from a HeNe laser was used for excitation of Raman scattering. SERS images and spectra were obtained at 2 s integration time with 6 mW laser output power by mapping an area of 100 μm × 100 μm (20 pixel × 20 pixel) using a 50× microscopy objective (N.A. = 0.75). A silicon wafer was used for calibration by checking the laser power at the sample and the focusing conditions based on the Raman intensity of the first-order phonon peak of silicon at *ca.* 520 cm^{-1}.

Results and discussion

Characterization of antibody–SERS label conjugates

Au/Ag-NS were prepared based on the template-engaged replacement reaction between silver nanoparticles and an aqueous solution of $HAuCl_4$ according to the procedure described by Xia and co-workers.[36,37] Their plasmon peak was tuned to ~630 nm for efficient SERS enhancement upon red laser excitation.[17,38] The as-prepared Au/Ag-NS were characterized by transmission electron microscopy (TEM) and extinction spectroscopy as shown in Fig. 2A and B, respectively. Their diameter is about ~60 nm and the corresponding plasmon peak is located at 628 nm. Scheme 1A depicts the synthesis of SERS-labeled antibodies starting from Au/Ag-NS. The modified Raman reporters Ra_1 and Ra_2 were obtained by covalent conjugation of monoethylene glycol (MEG–OH) and triethylene glycol (TEG–CO_2H) moieties to the nitro aromatic disulfide, 5,5′-dithiobis(2-nitrobenzoic acid) (DTNB). The hydrophilic stabilization approach enhances the water solubility of the noble metal colloid coated with a SAM of Ra_1 and Ra_2. This stabilization is independent of the actual Ra precursor and, more importantly, allows the subsequent conjugation with biomolecules after activation of the carboxyl group at the terminus of the longer spacer moiety (TEG–CO_2H) in Ra_2. A stoichiometric ratio of $Ra_1 : Ra_2 = 100 : 1$ was chosen to ensure the steric accessibility of the carboxyl groups in the densely packed SAM.[19,20,39] The addition of DTNB–MEG–OH (Ra_1) and DTNB–TEG–CO_2H (Ra_2) to the metal colloid leads to a hydrophilically stabilized self-assembled monolayer comprising two different terminal spacer units (dual spacer-SAM, *cf.* Fig. 1B). The presence of a close and dense packing of Raman reporter molecules within the SAM on the metal surface minimizes the co-adsorption of other molecules from the surrounding onto the metal surface (no spectral interference) and ensures the

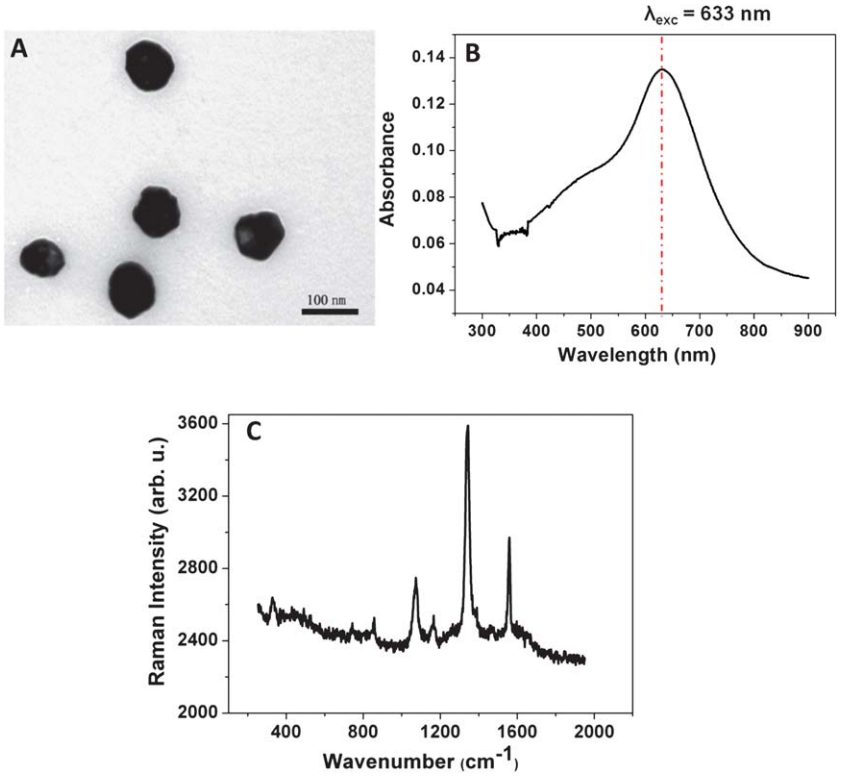

Fig. 2 TEM image (A), extinction spectrum (B) and SERS spectrum (C) of hydrophilically stabilized Au/Ag-NS.

maximum coverage of the metal surface with Raman reporter molecules (high sensitivity).[18,40] The carboxyl groups in the SAM on the surface of the Au/Ag-NS are activated by EDC/s-NHS for bioconjugation to antibodies. The bioconjugation step was confirmed and optimized by ELISA using an enzyme-labeled antibody (see the Experimental part for details). The SERS spectrum of the hydrophilically stabilized colloid (Fig. 2C) obtained upon red laser excitation (633 nm) exhibits a dominant peak at 1334 cm^{-1}, which is assigned to the symmetric stretching vibration of the nitro moiety in the nitro aromatic thiol.[18,19] The plasmon peak of the Au/Ag-NS exhibits a red-shift from 628 nm to 633 nm after coating with the SAM and further to 636 nm after EDC/s-NHS activation and bioconjugation to the antibody (Fig. S1A†). The similarity of the SERS spectra recorded after each functionalization step (Fig. S1B†) demonstrates the stability of the SERS NPs, in particular the stability of the SAM on the metal surface.

Stability of SERS labels under physiologically relevant conditions

High stability of SERS labels under physiologically relevant conditions is a necessary prerequisite for their successful application in bioanalytical chemistry. We therefore tested the stability of SAM-coated metal colloids against aggregation in various dispersion media. The extinction spectra in Fig. 3A indicate that hydrophilically stabilized SERS particles coated with Ra_1 (MEG–OH) are stable in water, HEPES buffer and even

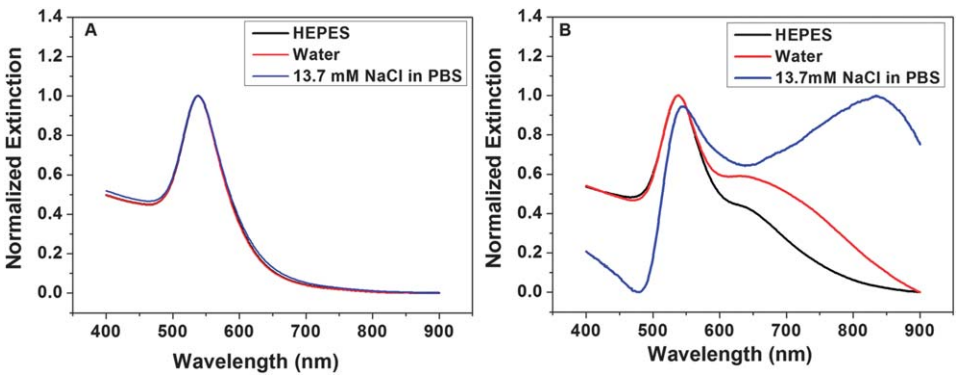

Fig. 3 Stability comparison between SERS labels with (A) and without a hydrophilically spacer (MEG–OH) conjugated to the Raman reporter moiety (B).

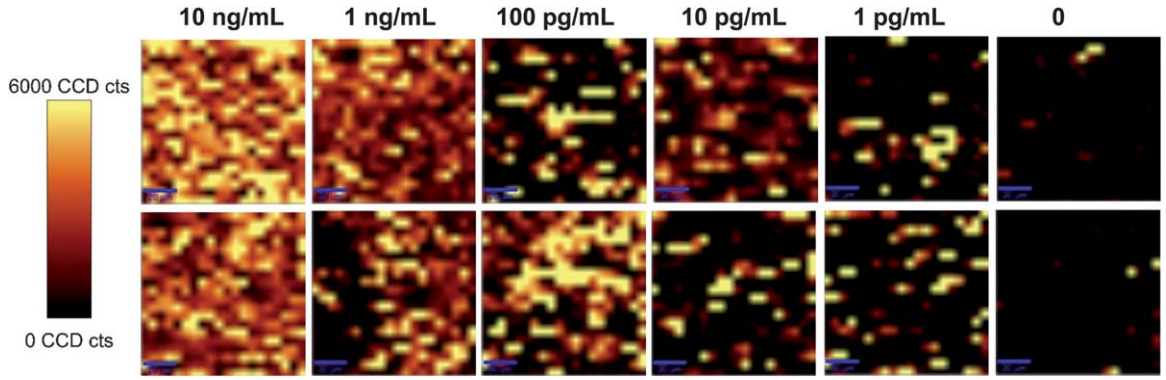

Fig. 4 Typical SERS false-color images recorded for different IL-6 concentrations ranging from 0 to 10 ng mL^{-1} using integrated Raman intensities in the range between 1330 and 1350 cm^{-1}.

in PBS buffer with high ionic strength (13.7 mM NaCl). In contrast, SERS labels without hydrophilic stabilization (no MEG–OH terminal in Ra_1) appear to be slightly aggregated in HEPES (50 mM) buffer and more strongly aggregated in water. The aggregation was worse in PBS buffer with 13.7 mM NaCl. Overall, these results demonstrate that the ethylene glycol spacer unit conjugated to the arylthiol as the actual Raman reporter moiety significantly increases the stability of SERS labels under physiologically relevant conditions, *i.e.*, buffer solutions with high ionic strength.

Detection of IL-6 using immuno-SERS microspectroscopy

Scheme 1B shows the procedure of the sandwich SERS immunoassay platform for IL-6 detection. Functionalized glass slides (*cf.* also Fig. S2†) were used for immobilizing the capture antibody. Sixteen different wells (reaction chambers/compartments) per glass slide were obtained by putting a commercially available polymer cover (photograph displayed in Scheme 1B). Eight pairs of wells were used for concentration-dependent SERS studies (C0–C5) including negative control experiments (BSA and casein). After blocking the surface with 2% BSA in PBST, the antigen (IL-6) is immobilized by specific binding to the capture antibody. Finally, the SERS-labeled detection antibody specifically recognizes the antigen at a different epitope, thereby forming the immuno-sandwich complex. Achieving reproducible data for biomolecular detection by SERS can be challenging due to the non-uniform spatial distribution of SERS nanoparticles on the surface.[41] This can be circumnavigated by averaging over SERS spectra recorded from different locations on the substrate.[9,10,38,42,43] However, this approach is usually limited to only a few positions which are arbitrarily chosen. In our study, a spatially resolved microspectroscopic SERS detection scheme (confocal Raman point mapping) is employed as the read-out method in order to obtain highly representative SERS spectra due to spatial averaging over larger areas including many pixels. Fig. 4 displays typical SERS false-color images using the integrated Raman intensity of the nitro moiety band of the Raman reporters between 1330 cm^{-1} and 1350 cm^{-1} in an area of 100 μm × 100 μm. For each IL-6 concentration in the range of 0–10 ng mL^{-1} (Fig. 4), two reaction chambers were analyzed (*cf.* Scheme 1B) by covering an area of 100 μm × 100 μm (20 × 20 = 400 pixels). Upon increasing the IL-6 concentration, more SERS-labeled detection antibodies bind to the glass surface, and consequently, a higher SERS intensity is detected, which is reflected in the brighter false-color SERS images. The SERS false-color images (Fig. 4) in combination with SEM images (Fig. S3†) indicate that it is difficult to achieve a very homogeneous distribution of the SERS nanoparticles on the surface, even though the fabrication and aggregation conditions of the hydrophilically stabilized colloid have been carefully controlled. Without the target antigen, only a very few single particles are observed, probably due to nonspecific binding, while at 100 pg mL^{-1} IL-6 more SERS particles are observed on the glass surface with slight aggregation (Fig. 4 and S3†). These observations stress the importance of averaging the SERS signal over larger areas instead of arbitrarily selecting only a few positions for signal acquisition.[44]

(a) Reproducibility and sensitivity of the IL-6 SERS immunoassay. To test the reproducibility of the SERS immunoassay, repeated experiments were conducted as shown in Figs. S4 and S5†. SERS false-color images and average SERS spectra for 1 ng mL^{-1} IL-6 were compared on the same day (Fig. S4†) and

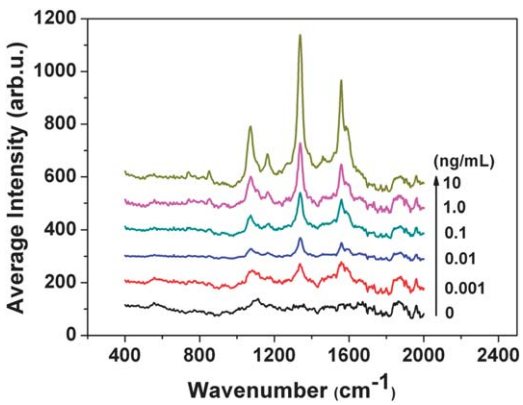

Fig. 5 SERS spectra for IL-6 detection at different concentrations. The SERS spectrum was obtained by the average of 2000 individual spectra in the SERS mapping.

different days (Fig. S5†). Thus, average SERS spectra were analyzed based on these images (thousands of points, individual spectra) as indicated in Fig. 5. The concentration-dependent SERS response curve in Fig. 6 is based on the average SERS spectra for each concentration in the range of 1 pg mL^{-1} to 1 μg mL^{-1}. Again, the integrated Raman intensity of the band around 1334 cm^{-1} from the Raman reporter was used for generating image contrast. The lowest detectable concentration for IL-6 is *ca.* 1 pg mL^{-1}, which is one to two orders more sensitive than the conventional ELISA.[33]

(b) Selectivity of the IL-6 SERS immunoassay. Specificity is also a very important feature of an immunoassay. In this study, 2% BSA, 2% casein and 1 μM protein G (much higher concentration than the target antigen) instead of IL-6 were used for negative control experiments. The diagram and average SERS spectra in Fig. 7 indicate only very weak SERS signals for BSA, casein and protein G, demonstrating the high specificity of the SERS immunoassay. Additional negative control experiments using SERS-labeled BSA and SERS-labeled antibodies directed against interleukin 8 (IL-8) were performed. Low SERS intensities are observed, similar to those observed in the absence of IL-6 (0 pg mL^{-1}), indicating nonspecific protein binding (BSA) and low cross reacting with a similar target (IL-8).

(c) Comparing the sensitivity for Au/Ag-NS to solid quasi-spherical Au-NPs. Solid quasi-spherical gold nanoparticles (Au-NPs) with the same diameter as the Au/Ag-NS (60 nm) were employed in the same sandwich immunoassay platform for comparing their performance as plasmonic materials for SERS detection. The same protocols for bioconjugation, incubation and SERS microspectroscopic mapping used for Au/Ag-NS were also applied for IL-6 detection with Au-NPs. Using the SERS false-color images obtained at different IL-6 concentrations (Fig. S6†), the SERS intensity *vs.* IL-6 concentration diagram in Fig. 8A was constructed. Based on the SERS response curve in Fig. 8, the lowest detectable concentration is *ca.* 10–100 pg mL^{-1}, which is one to two orders of magnitude worse compared with the Au/Ag-NS. This is due to the higher scattering efficiency of Au/Ag-NS compared with Au-NPs.[14] The extinction spectra in Fig. S7† contain the sum of both scattering and absorption contributions and exhibit plasmon peaks at 540 nm (Au-NPs)

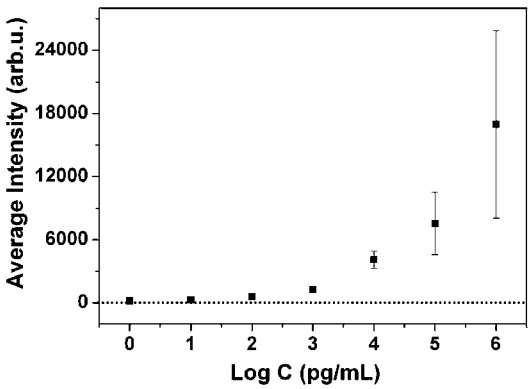

Fig. 6 Average SERS intensity as a function of IL-6 concentration detection in the range from 1 pg mL^{-1} to 1 μg mL^{-1}.

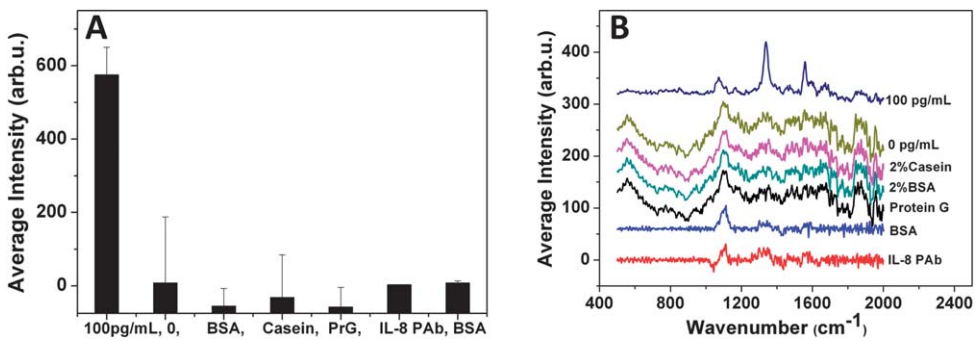

Fig. 7 SERS intensity (A) and average SERS spectrum (B) for testing the specificity of the IL-6 sandwich immunoassay using Au/Ag-NS.

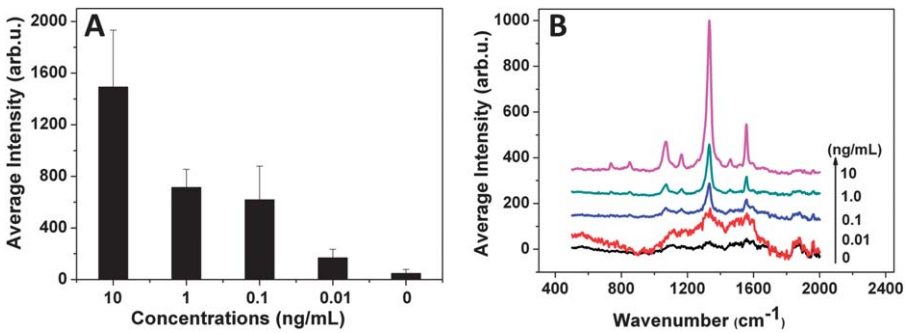

Fig. 8 SERS intensity (A) and average SERS spectrum (B) for the IL-6 sandwich immunoassay using solid quasi-spherical Au-NPs.

and 628 nm (Au/Ag-NS), respectively. The green line in Fig. S8† shows the laser excitation wavelength used in this study (633 nm), while the blue line indicates the Stokes–Raman wavelength corresponding to the marker band of the Raman reporter at 1334 cm^{-1} (691 nm).[45] Since the Stokes-SERS intensity is strongly dependent on the scattering cross-sections at the wavelength of both the incident laser and the Stokes–Raman scattering, it was calculated that the enhancement of Au/Ag-NS is about 20 times larger than that for Au-NPs at red laser excitation (633 nm).[17] Our experimental finding of the improved SERS sensitivity of Au/Ag-NS compared with Au-NPs in an IL-6 SERS immuno-sandwich assay confirms this theoretical prediction.

Conclusions

In the present study, rationally designed Au/Ag-NS were employed as SERS labels for the sensitive and selective detection of the cytokine IL-6. The Raman reporter moieties were conjugated to ethylene glycol spacers with terminal OH and CO_2H groups and are present as a SAM on a nanoshell surface. This hydrophilically stabilized dual-spacer SAM on Au/Ag-NS exhibits a high stability, even under physiologically relevant conditions such as buffer solutions with high ionic strength. The hydrophilically stabilized colloid does not precipitate, while the non-stabilized colloid precipitate. The lowest detectable concentration for IL-6 is *ca.*1 pg mL^{-1} with Au/Ag-NS, which is at least one order of magnitude better than for hydrophilically stabilized, nonaggregated solid Au-NPs of the same size. Owing to the high signal strength and specificity for IL-6 detection with these rationally designed plasmonic nanostructures for red laser excitation, it is expected that the detection of IL-6 also in human samples such as plasma and blood samples for clinical diagnostics can be achieved, preferably with portable Raman instrumentation.

Acknowledgements

Financial support from the Alexander von Humboldt Foundation, the State of Lower Saxony (EFRE/W2-80111700), and the German Research Foundation (DFG, INST 190/128-1) is acknowledged.

References

1 D. Graham, K. Faulds and W. E. Smith, *Chem. Commun.*, 2006, **42**, 4363–4371.
2 W. E. Doering, M. E. Piotti, M. J. Natan and R. G. Freeman, *Adv. Mater.*, 2007, **19**, 3100–3108.
3 S. Schlücker, in *Surface-Enhanced Raman Spectroscopy: Analytical, Biophysical and Life Science Applications*, ed. S. Schlücker, Wiley-VCH, Weinheim, Germany, 2011, pp. 263–283.
4 Y. C. Cao, R. C. Jin, J. M. Nam, C. S. Thaxton and C. A. Mirkin, *J. Am. Chem. Soc.*, 2003, **125**, 14676–14677.
5 Y. W. C. Cao, R. C. Jin and C. A. Mirkin, *Science*, 2002, **297**, 1536–1540.
6 D. Graham, B. J. Mallinder, D. Whitcombe, N. D. Watson and W. E. Smith, *Anal. Chem.*, 2002, **74**, 1069–1074.
7 M. D. Porter, R. J. Lipert, L. M. Sioperko, G. Wang and R. Narayanan, *Chem. Soc. Rev.*, 2008, **37**, 1001–1011.
8 J. Ni, R. J. Lipert, G. B. Dawson and M. D. Porter, *Anal. Chem.*, 1999, **71**, 4903–4908.
9 D. S. Grubisha, R. J. Lipert, H. Y. Park, J. Driskell and M. D. Porter, *Anal. Chem.*, 2003, **75**, 5936–5943.
10 G. F. Wang, R. J. Lipert, M. Jain, S. Kaur, S. Chakraboty, M. P. Torres, S. K. Batra, R. E. Brand and M. D. Porter, *Anal. Chem.*, 2011, **83**, 2554–2561.
11 G. F. Wang, H. Y. Park, R. J. Lipert and M. D. Porter, *Anal. Chem.*, 2009, **81**, 9643–9650.
12 S. Xu, X. Ji, W. Xu, X. Li, L. Wang, Y. Bai, B. Zhao and Y. Ozaki, *Analyst*, 2004, **129**, 63–68.
13 X. X. Han, Y. Kitahama, T. Itoh, C. X. Wang, B. Zhao and Y. Ozaki, *Anal. Chem.*, 2009, **1**, 3350–3355.
14 X. X. Han, B. Zhang and Y. Ozaki, *Anal. Bioanal. Chem.*, 2009, **394**, 1719–1727.
15 M. E. Pekdemir, D. Ertürkan, H. Külah, I. H. Boyaci, C. Ozgen and U. S. Tamer, *Analyst*, 2012, **137**, 4834–4840.
16 B. Guven, N. Basaran-Akgul, E. Temur, U. Tamer and I. H. Boyaci, *Analyst*, 2011, **136**, 740–748.
17 B. Küstner, M. Gellner, M. Schütz, F. Schöppler, A. Marx, P. Ströbel, P. Adam, C. Schmuck and S. Schlücker, *Angew. Chem., Int. Ed.*, 2009, **48**, 1950–1953.
18 C. Jehn, B. Küstner, P. Adam, A. Marx, P. Ströbel, C. Schmuck and S. Schlücker, *Phys. Chem. Chem. Phys.*, 2009, **11**, 7499–7504.
19 S. Schlücker, M. Salehi, G. Bergner, M. Schütz, P. Strobel, A. Marx, I. Petersen, B. Dietzek and J. Popp, *Anal. Chem.*, 2011, **83**, 7081–7085.
20 M. Schütz, D. Steinigeweg, M. Salehi, K. Kömpe and S. Schlücker, *Chem. Commun.*, 2011, **47**, 4216–4218.
21 B. J. Yakes, R. J. Lipert, J. P. Bannantine and M. D. Porter, *Clin. Vaccine Immunol.*, 2008, **15**, 227–234.
22 J. L. Gong, Y. Liang, Y. Huang, J. W. Chen, J. H. Jiang, G. L. Shen and R. Q. Yu, *Biosens. Bioelectron.*, 2007, **22**, 1501–1507.
23 K. Chen, H. Han and Z. Luo, *Analyst*, 2012, **137**, 1259–1264.
24 R. Thorpe, M. Wadhwa, C. R. Bird and A. R. Mire-Sluis, *Blood Rev.*, 1992, **6**, 133–148.
25 T. L. Whiteside, *J. Clin. Immunol.*, 1994, **14**, 327–339.
26 S. Laing, A. Hernandez-Santana, J. Sassmannshausen, D. L. Asquith, I. B. McInnes, K. Faulds and D. Graham, *Anal. Chem.*, 2011, **83**, 297–302.
27 Y. Dowlati, N. Herrmann, W. Swardfager, H. Liu, L. Sham, E. K. Reim and K. L. Lanctot, *Biol. Psychiatry*, 2010, **67**, 446–457.
28 O. P. Kristiansen and T. Mandrup-Poulsen, *Diabetes*, 2005, **54**, S114–124.
29 W. Swardfager, K. Lanctôt, L. Rothenburg, A. Wong, J. Cappell and N. Herrmann, *Biol. Psychiatry*, 2010, **68**, 930–941.
30 P. C. Smith, A. Hobisch, D. L. Lin, Z. Culig and E. T. Keller, *Cytokine Growth Factor Rev.*, 2001, **12**, 33–40.
31 N. Nishimoto, *Curr. Opin. Rheumatol.*, 2006, **18**, 277–281.

32 Cancer Patients Typically Have Increased Interleukin-6 Levels. American Society of Clinical Oncology 2006 Annual Meeting, Abstracts 8632 and 8633, http://Medscape.com, 2006-06-26.
33 ELISA kit for IL-6 detection, http://www.sinobiological.com/IL6-IFNB2-ELISA-kit-g-2677.html.
34 W. Tan, L. Sabet, Y. Li, T. Yu, P. R. Klokkevold, D. T. Wong and C. M. Ho, *Biosens. Bioelectron.*, 2008, **24**, 266–271.
35 T. Yamaguchi, T. Kaya, M. Aoyama and H. Takei, *Analyst*, 2009, **134**, 776–783.
36 Y. G. Sun, B. T. Mayers and Y. N. Xia, *Nano Lett.*, 2002, **2**, 481–485.
37 Y. Sun and Y. Xia, *Anal. Chem.*, 2002, **74**, 5297–5305.
38 S. W. Bishnoi, Y. J. Lin, M. Tibudan, Y. Huang, M. Nakaema, V. Swarup and T. A. Keiderling, *Anal. Chem.*, 2011, **83**, 4053–4060.
39 M. Schütz, C. Müller, M. Salehi, C. Lambert and S. Schlücker, *J. Biophotonics*, 2011, **6**, 453–463.
40 M. Gellner, K. Kömpe and S. Schlücker, *Anal. Bioanal. Chem.*, 2009, **394**, 1839–1844.
41 R. A. Tripp, R. A. Dluhy and Y. Zhao, *Nano Today*, 2008, **3**, 31–37.
42 C. C. Lin, Y. M. Yang, Y. F. Chen, T. S. Yang and H. C. Chang, *Biosens. Bioelectron.*, 2008, **24**, 178–183.
43 C. Song, S. Z. Wang, R. Zhang, J. Yang, X. Tang and Y. Cui, *Biosens. Bioelectron.*, 2009, **25**, 826–831.
44 M. Lee, S. Lee, J. Lee, H. Lim, G. H. Seong, E. K. Lee, S. Chang, C. H. Oh and J. Choo, *Biosens. Bioelectron.*, 2011, **26**, 2135–2141.
45 M. Gellner, B. Küstner and S. Schlücker, *Vib. Spectrosc.*, 2009, **50**, 43–47.